Microfluidics Nanofluidics manuscript No.
(will be inserted by the editor)

A polymeric high-throughput pressure-driven micromixer using a nanoporous membrane

Oliver Jännig · Nam-Trung Nguyen ·

Abstract This paper presents a polymeric high-throughput, pressure-driven nanofluidic mixer utilizing a nanoporous charge-selective Nafion membrane. The device has no movable parts and is fabricated in PMMA by means of laser machining and thermal bonding. Mixing is achieved by strong vortices occurring above the nanoporous membrane when applying an electric field. These vortices are caused by electroconvection in the concentration polarization zone. The mixer is operating at Peclet number as high as 63.5×10^3 allowing rapid mixing at a high throughput. The design and fabrication of

O. Jänig

Faculty of Electrical Engineering and Information Technology

Chemnitz University of Technology

Reichenhainer Str. 70, Chemnitz, Germany 09126

N. T. Nguyen

School of Mechanical and Aerospace Engineering

Nanyang Technological University

50 Nanyang Avenue, Singapore, Singapore 639798

Tel.: +65-6790-4457

Fax: +65-6792-4062

E-mail: mntnguyen@ntu.edu.sg

the mixer is simple, reproducible and of low cost. The fabrication approach presented in this paper can be easily transferred to roll-to-roll technology for mass fabrication.

Keywords Micromixer · nanofluidics · electrokinetics · polymeric micromachining · instability

1 Introduction

Mixing plays an important role in many microfluidic devices. Micro Total Analysis Systems (TAS) or Lab-on-Chip (LOC) devices require this function to be integrated for applications such as medical diagnostics, genetic sequencing, proteomics or drug discovery [1]. Due to the small channel size, laminar flow condition exists in almost all microfluidic devices. In these applications, the Reynolds number representing the ratio between inertial force and friction force is usually smaller than unity. Two different fluids can only mix by molecular diffusion at their interface. The Peclet number representing the ratio between advective transport and diffusive transport is typically more than one thousand in most microfluidic applications. Thus, advective mass transport dominates diffusive mass transport in micro scale [2]. A very long mixing channel would be needed if mixing relies entirely on molecular diffusion. Increasing the interfacial area by chaotic advection or inducing disturbances can decrease the length of the mixing channel tremendously [3]. Inducing disturbances with electric field is relatively easy to implement due to the simple integration of electrodes into a microfluidic device. Oddy et al. used oscillating electro-osmotic flow induced by an AC voltage to improve mixing in a microchannel [4]. Tang et al. switched alternately the electro-osmotic flows to create segments of the fluids to be mixed along the flow direction [5]. In a microfluidic system driven by electroosmosis, instability can be induced by the imbalance between

electroosmotic force and electroviscous force. Electroosmotic force is a surface force created at the double layer, while electroviscous force is a body force caused by the charge gradient in the bulk fluid. Instability can therefore induced by a gradient in conductivity [6], and variation of zeta potential [7,8].

Concentration polarization (CP) above a nanoporous membrane or next to a nanochannel creates a space charge inside the CP zone. Under an electric field, this charge creates liquid flow along the surface. The flow velocity generated by this phenomenon can be one or two order of magnitudes larger than the Smoluchowsky's velocity created by the electric double layer [9]. This phenomena is called electroconvection in concentration polarization [10,11]. More importantly, the direction of the flow induced by electroconvection in CP is not constrained by the direction of the applied electric field. The transversal components of this flow can be used for improved mixing in microchannel. Rubinstein and Zaltzman investigated this phenomenon above a permselective membrane [10]. The voltage/current curve of a persmelective cation exchange membrane is characterized by three regions: ohmic, limiting and overlimiting regions. Due to the established ion depletion zone, the current remains almost constant at increasing voltage in the limiting region. In the overlimiting region, the current increases with increasing voltage. In this region, the current is fluctuating due to strong vortices generated by electroconvection in CP. Analytical analysis by Zaltzman and Rubinstein [11] showed that the linear velocity of the vortex is proportional to the square of the applied voltage. This relationship was confirmed experimentally by Kim et al. with nanochannels fabricated in silicon [12]. The strong vortices next to the nanochannels were used by Kim et al. to realise a micromixer with mixing index ranging from 0.7 to 0.8 [12]. The liquid in this mixer was driven by electroosmosis. Kuo et al. [13] mixed two electrokinetically driven flows using a nanoporous membrane. The two microchan-

nels are separated by the membrane. The liquids to be mixed are transported across the membrane. This work did not used the induced flow near the membrane to mix the liquid. Due to the relatively low electrokinetic flow rate, the Peclet number in the above works [12, 14] with nanochannels is on the order of 100. The low flow rate also makes practical mixing applications not possible. Generally, the use of deterministic nanochannels, which need to fabricated, is not practical for mixing in microscale. Due to the limited number of nanochannels, blockage by particles presents a real problem for practical use of nanochannels for mixing. Fabricated nanochannels can be easily be filled by capillarity and dried by evaporation. After evaporation, the residues of species previously dissolved in the liquid remain in the nanochannels and cause the blockage. Due to this problem, devices with nanochannels often need to be kept in a wetted state before the experiments, and the experiment can only be carried out once. Nanoporous membrane presents a practical solution for the blockage problem. Due to the unlimited nano pathways in the membrane, blockage at a few places on the membrane would not affect the functionality of the microfluidic device. Devices using nanoporous membranes can be used repeatedly with high reproducibility. Polymer electrolyte membrane fuel cell (PEMFC) is the evidence for the practical use of nanoporous membrane.

In this paper we apply the concept of induced electroosmosis near a nanoporous membrane to a pressure-driven micromixer. The mixer works with Peclet number on the order of 10^3 making high-throughput applications possible. Furthermore, we employed a low-cost and simple technology to take advantage of nanofluidic phenomena without the need of fabricating the nanochannels [15]. The fabrication process reported here can be easily transferred to roll-to-roll lamination technology for mass fabrication. The mixer design presented in this paper can be numbered up to achieve even higher throughput. The device concept presented here can be used for practical implementa-

tion of other applications utilizing nanochannels such as sample concentration. Another application of CP is desalination [16]. The device concept presented here can be use for the implementation of a desalination apparatus at a reasonable cost. Following, the design, fabrication, and characterisation of the mixer are presented and discussed.

2 Device Concept and Fabrication Technology

2.1 Device Concept

Figure 1 shows the schematic concept of the nanofluidic mixer. The device consists of a coiling microchannel with two inlets and one outlet. The mixing channel is designed in the way that it turns and crosses itself near the entrance. These crossing parts of the mixing channel are connected through a nanoporous Nafion membrane, Fig. 1(a). Nafion is cation selective and repels negative charges. Figure 1(b) shows the three typical regions of the voltage-current curve of a cation-exchange membrane. The microchannel guides the bulk flow and the nanoporous membrane acts as a barrier for generating the ion-depletion zone. If an external voltage is applied from the inlets to the outlet along the flow direction, overlapping normal and tangential electrical fields exist on the surface of the nanoporous membrane. A concentration polarisation (CP) zone develops above the nanoporous membrane, Fig. 1(b). Strong vortices are induced in the region above the nanoporous membrane. The vortices promote mass transport in transversal direction and increase the interfacial area between the incoming fluids, and hence rapidly mix them.

2.2 Fabrication Technology

The above concept was implemented in a polymeric device. Polymethylmethacrylate (PMMA) sheets with thicknesses of 0.25 mm and 3 mm were purchased from Good Fellow (Cambridge, UK). The nanoporous Nafion film (NRE-211) was purchased from DuPont (USA). The mixer is assembled by lamination of the five PMMA layers, Figure **??**(a). Layers 2 to 5 are made of 0.25-mm thick PMMA sheets. The microchannels are cut through in layers 2 and 4. Layer 3 has a cavity to embed the rectangular nanoporous membrane. The contact slit is opened in layer 3. Layer 5 contains the access holes for the inlets and the outlet. Layer 1 is made of a 3-mm thick PMMA substrate to provide a rigid support for the entire device. Each layer was designed with commercial software (CorelDraw X3) and transferred to a laser cutter (Universal M-300, Universal Laser Systems Inc.). The cutting system has a 25 W CO_2-laser with a maximum beam speed of 640 mm/s. The channels and the slit were cut through the 0.25 mm PMMA sheet using a power of 4.75 W and a scanning speed of 19 mm/s. The 60-μm deep cavity for the nanoporous membrane was ablated using a lower power of 0.5 W and a scanning speed of 13 mm/s. The same laser was also used to cut out the 2 mm$\times$3 mm piece of Nafion.

With the help of an injection needle, fast hardening cyanoacrylate adhesive (Permabond, PA, USA) was applied onto the cavity to position the membrane and make its borders leak proof. The membrane was placed into the cavity manually. Because the membrane instantly bends when exposed to the glue, two tweezers were used to hold down all four corners. Subsequently, the 3-mm thick bottom layer and the four 0.25-mm thick PMMA layers were bonded in a single thermal bonding process using a hot press (Carver Manual Press 4386). The press consists of two hotplates and a

hydraulic pump to create the required bonding pressure. The PMMA stack was placed between two metal templates. A polydimethylsiloxane (PDMS) piece was placed under the upper plate to compensate a small angular displacement of the hotplates and hence to achieve equal pressure distribution on the PMMA stack. At a pressure of 0.86 MPa the plates were heated from room temperature (24°C) to 110°C within seven minutes. For twelve minutes the hotplates were kept at 110°C. To avoid thermal stress, the setup was cooled with a fan to 40°C within 45 minutes. After releasing the bonded chip, 100-μm thick platinum wires were fixed with adhesive tape near the fluid inlets to work as elctrodes. Injection needles (BD Precission Glide 25G 1") were glued to the inlets and outlet of the device by a two-component epoxy adhesive (OCI Fast Set 4 Min. Epoxy, FL, USA). In this manner, the platinum wires were permanently positioned and sealed.

Figure 2(b) shows the assembled device. The final device measures 30 mm by 38 mm. The thick bottom layer maintains the mechanical integrity of the entire device. At the same time, a thick bottom layer allows the later investigation with an inverted microscope. During the thermal bonding process, the pattern of the hotplate was slightly embossed onto the adjacent polymer surfaces. Since optical access is from the bottom of the device, a thick bottom layer can remove the embossed pattern out of the focal point of the microscope. The height, width and total length of the mixing channel are 0.25 mm, 0.4 mm and 37.3 mm, respectively. The cavity for the 50-m thick Nafion membrane measures 3 mm by 2 mm and is about 60 μm in depth. The contact slit in the cavity measures approximately 0.1 mm in width and 0.6 mm in length to overlap the entire width of the mixing channel.

3 Experiments

The mixing process was characterized with the help of an inverted epi-fluorescent microscope (Nikon Eclipse TE2000-S). The fluidic inlets were connected to a syringe (BD 5ml) via tubings (Tygon S-54-HL). The desired flow rates were adjusted using a syringe pump (Cole-Parmer, 74900-05, 0.2 μl/h-500 μl/h, accuracy of 0.5%). The platinum wires were connected to a high voltage supply (Model PS350, Stanford Research System, Inc). The fluids in use were de-ionised (DI) water from MiliQ system (grade 1, ultra pure water, 18.2 M $\cdot$cm at 25°C, Millipore, MA, USA) and DI water with a flourescent dye. Rhodamine B ($C_{28}H_31N_2O_3Cl$, Sigma Aldrich) was used as the neutral fluorescent dye in our experiment. Rhodamine B is neutrally charged, and it does not affect the ion concentration and the electroosmotic effect. While varying the applied voltage and the flow rate, images of the fluorescence intensity were captured using an interline transfer charge-coupled device CCD camera (HiSense MkII). The mixing behaviour or the concentration distribution of the fluorescent dye is directly related to the distribution of the intensity values. The resolution of the CCD camera is 1344×1024 pixels with 12 bit grayscale. An excitation wavelength of 540-nm and a maximum emission wavelength of 610 nm were imaged with the epifluorescent attachment of type Nikon G-2E/C (excitation filter for 540 nm, dichroic mirror for 565 nm, and an emission filter for 605 nm). Videos was recorded by a commercial camcorder (Sony, DCR-DVD803E) attached to the eyepiece of the microscope.

An image processing software (ImageJ, NIH, USA) was used to extract the grayscale values of the images to a database. The data was then imported into a professional mathematical software (Mathcad14). Intensity values $I^*_{\max}$ and $I^*_{\min}$ of the unmixed liquids at the inlets were extracted and taken as reference for the maximum and mini-

mum intensity values for DI water and the fluorescent solution. All intensity data was normalized to values between 0 and 1:

$$I_i = \frac{I_i^* - I_{\min}^*}{I_{\max}^* - I_{\min}^*} \tag{1}$$

where I_i^* is the actual intensity value of pixel i, $I_{\max}^*$ and $I_{\min}^*$ are the maximum and minimum intensity values of the unmixed liquids. The mixing behaviour was observed at cross sections about 0.8 mm upstream and downstream of the nanoporous slit as indicated in Fig. 3(a). The mixing efficiency η_{mixing} mixing was used to quantify the degree of mixing:

$$\eta_{\text{mixing}} = 1 - \frac{MI}{MI_{\text{nomixing}}} \tag{2}$$

with the mixing index:

$$MI = \sqrt{\frac{1}{N}\sum_{i=1}^{N}\left(\frac{I_i - \bar{I}}{\bar{I}}\right)^2} \tag{3}$$

wherein N is the number of pixels to be evaluated, I_i is the actual normalized grayscale value of pixel i, and $\bar{I} = 0.5$ is the expected normalized grayscale value for perfect mixing. The mixing index of non mixed streams is evaluated as:

$$MI_{\text{nomixing}} = \sqrt{\frac{1}{N}\sum_{i=1}^{N}\left(\frac{I_{\text{min,max}} - \bar{I}}{\bar{I}}\right)^2} \tag{4}$$

where $I_{\text{min,max}}$ can be either 0 or 1. Experiments were carried out for voltages up to 2.6 kV and at four flowrates of 20, 40, 200 and 400 μl/min. The corresponding Reynolds number:

$$\text{Re} = \frac{\rho U D_{\text{h}}}{\mu} \tag{5}$$

and Peclet number:

$$\text{Pe} = \frac{UW}{D} \tag{6}$$

listed in Table 1 are estimated with properties (density ρ, dynamic viscosity μ) of water and a diffusion coefficient of Rhodamine B of $D = 4.2 \times 10^{-10}$ m^2/s [17]. In

Table 1 Flow rates under investigation and corresponding average velocity, Reynolds number and Peclet number for Rhodamine B.

Flow rate (μl/min)	Average velocity (mm/s)	Re	Pe ($\times 10^3$)
20	3.33	1.03	3.17
40	6.67	2.05	6.35
200	33.3	10.3	31.7
400	66.7	20.5	63.5

equations (5) and (6), U, D_{h} and W are the average velocity, the hydraulic diameter and the width of the mixing channel, respectively. In contrast to all previous works on electroconvection in concentration polarization, we are working with relatively high Reynolds number and Peclet number.

4 Results and Discussion

Figure 3 shows representative intensity images of the mixer. Without the applied voltage, the fluids follow the mixing channel and cross the entrance region after the turn. It is to note that the returning flow appears to be fully mixed with a homogenous intensity image, Fig. 3(a). In fact, because of the high Peclet number, the two streams still flow side by side but overlap in the viewing direction, Fig. 1(a). The overlapping streams makes the intensity image appear to be homogenous. With increasing voltage, a CP zone develops above the nanoporous membrane connecting the two crossing microchannels. Mixing downstream of the nanoporous membrane is visible, Fig. **??**(b). The zone of concentration polarization is located above and around the membrane area. Its shape is affected by the pressure driven flow. As illustrated in Figure 1(a), the zone downstream is expected to be larger due to advection caused by the pressure driven flow. An increasing voltage enlarges the CP zone. At a voltage high enough for

the velocity of the vortices to overcome the hydrodynamic velocity, the CP zone can reach the Y-junction at the entrance. Rapid mixing occurs as soon as the two fluids meet.

Figure 4 shows the mixing efficiency at the downstream position as function of the applied voltage. Without the electric field, a low mixing efficiency is achieved by diffusive mixing. A higher flow rate means a larger Peclet number and negligible diffusive mixing across the channel width. This fact is reflected well by the mixing efficiency at $V = 0$. A higher flow rate results in a lower mixing efficiency, Fig. 4. The mixing efficiency increases with increasing voltage. The current passing through the nanoporous membrane forms a ion-depletion or CP zone. The size of the zone and the extent of the vortices correlate with the current passing through the nanoporous membrane. Thus, mixing efficiency measured downstream of the membrane also correlates with this current. At a low flow rate the phenomenon of electroconvection in concentration polarization dominates over the advection of the pressure driven flow. The mixing efficiency versus voltage curve follows the typical behaviour of the voltage-current curve of a cation exchange membrane as depicted in Fig. 1(b). In Fig. 4, the mixing efficiency curves of 20 μl/min and 40 μl/min reaches a plateau corresponding to the limiting region followed by a sharp increase corresponding to the overlimiting region. At higher flow rates of 200 μl/min and 400 μl/min, the pressure driven flow increases advection in flow direction and limits the transversal transport caused by the vortices. For the same applied voltage, mixing efficiency is lower at a higher flow rate. However, the plateau and the sharp increase in mixing efficiency can still be observed at these high flow rates.

Figure 5 shows the mixing efficiency at different flow rates measured upstream of the Nafion membrane. Due to advection caused by the pressure driven flow, the CP zone

and the vortices can not reach the upstream position at low applied voltages. For each flow rate, there is a threshold voltage where the mixing efficiency increases dramatically. Beyond this threshold voltage, the mixing efficiency jumps from that of diffusive mixing to the corresponding level measured down stream (Fig. 4). To grow against the pressure driven flow, the linear velocity of the vortices should be larger than the pressure-driven velocity. Thus, at the threshold voltage the magnitude of the velocity of the vortices should be the same as that of the pressure-driven hydrodynamic velocity. To confirm this hypothesis, the threshold voltage is plotted against the corresponding flow rate in Figure 6. Exponential fitting shows that the threshold voltage is almost a square root function of the flow rate. That means indirectly that the linear velocity of the vortices is proportional to the square of the applied voltage. Previous theoretical and experimental works by Rubinstein and Zaltzman[10] as well as Kim et al.[12] led to the same conclusion.

To estimate the error of the measured mixing efficiency, the intensity values for DI water and Rhodamine B solution were measured at the inlets, i.e. before the two streams join. The relative error of the fluorescent solution is approximately twice as high as that of water. The relative error of the mixing efficiency ranges from 5% to 13% depending on the degree of mixing. In no mixing situation of a side-by-side flow, the error is low. In a fully mixed stream every point of the cross section contains fluorescence resulting in a higher error.

5 Conclusions

This paper reports the fabrication and characterisation of a high-throughput ultra-rapid mixer with no movable parts. A simple, fast and low-cost fabrication technology

was reported. The layer-by-layer design and the lamination approach can be transferred to roll-to-roll technology promising low-cost and large-scale manufacturing of the device. Nanoscale pores and channels are fundamental for the working concept of the mixer. These nanostructures were implemented by integrating a commercially available nanoporous membrane in a stack of PMMA films. All parts were cut and machined with the same laser platform. A single thermal bonding process was sufficient to laminate the different device layers to a functional mixer. The characterisation shows good mixing results. Due to the strong vortices, as soon as the zone of concentration polarisation covers the entire channel cross section, the two streams can be considered as fully mixed. If the CP region expands until the Y-junction the two fluids mix immediately when they first meet. The device works with a throughput as high as 400 μl/min. The corresponding Peclet number is 63.5×10^3. The presented device can achieve the same mixing index between 0.7 and 0.8 as achieved previously by the micromixer with deterministic nanochannels [14]. In our future works, the mixer design needs to be optimized and characterised. The channel length can be further reduced to decrease the voltage needed for mixing. The electrodes can be placed closer to the nanoporous membrane to reduce the voltage. Our preliminary tests with another nanoporous membrane were successful. In this case, the Nafion membrane was replaced by a track-etched nanoporous polycarbonate membrane. The results show that a device made of a single polymeric material such as polycarbonate is possible. Furthermore, we will apply the same device concept to implement a desalination device which can be fabricated on a large surface and at a low cost using the roll-to-roll lamination technology.

Acknowledgement

OJ would like to acknowledge the support of Fraunhofer Research Institute for Electronic Nano Systems (ENAS) for his 6-month research attachment at NTN's lab. NTN would like to acknowledge the support of SMART Innovation Centre for the grant ING09007 "Water Purification for Remote Location".

References

1. Nguyen N.T. and Z.G. Wu, "Micromixers - a review". Journal of Micromechanics and Microengineering, **15,** R1–R16 (2005).
2. Wu Z.G. and N. T. Nguyen, "Convective-diffusive transport in parallel lamination micromixers". Microfluidics and Nanofluidics, **1,** 208–217(2005).
3. Wu Z.G. and N. T. Nguyen, "Rapid mixing using two-phase hydraulic focusing in microchannels". Biomedical Microdevices, **7,** 13–20 (2005).
4. Oddy M.H., J.G. Santiago and J.C. Mikkelsen, "Electrokinetic instability micromixing". Analytical Chemistry, **73,** 5822–5832 (2001).
5. Tang Z., S. Hong, D. Djukic, V. Modi, A.C. West, J. Yardley and R.M. Osgood, "Electrokinetic flow control for composition modulation in a microchannel". Journal of Micromechanics and Microengineering, **12,** 870–877 (2001).
6. Posner, J.D and J.G Santiago, "Convective instability of electrokinetic flows in a cross-shaped microchannel". Journal of Fluid Mechanics, **555** 1–42 (2006).
7. Lin J.L., K.H. Lee and G.B. Lee, "Active mixing inside microchannels utilizing dynamic variation of gradient zeta potential s". Electrophoresis, **26** 4605–4615 (2005).
8. Biddiss E., D. Erickson and D. Li, "Heterogeneous surface charge enhanced micromixing for electrokinetic flows". Analytical Chemistry, **76** 3208–3213 (2004).
9. Mishchuk N.A. and P.V. Takhistov, "Electroosmosis of the second kind". Colloids Surfaces A: Physicochem. Eng. Aspects, **95** 119–131 (1995).
10. Rubinstein I. and B. Zaltzman, "Electro-osmotically induced convection at a permselective membrane". Physical Review E, **62** 2238–2251 (2000).

11. Zaltzman B., I. Rubinstein, "Electro-osmotic slip and electroconvective instability". Journal of Fluid Mechanics, **579** 173–226 (2007).

12. Kim S.J., Y.C. Wang, J. H. Lee, H.C. Jang and J.Y. Han, "Concentration polarization and nonlinear electrokinetic flow near a nanofluidic channel". Physical Rreview Letters, **99** 044501 (2007).

13. Kuo T.-C., H.-K. Kim, D.M. Cannon Jr., M.A. Shannon, J.V. Sweedler and P.W. Bohn, "Nanocapillary arrays effect mixing and reaction in multilayer fluidic structures". Angewandte Chemie - International Edition, **43** 1862–1865 (2004)

14. Kim D.J., A. Raj, L.K. Zhu, R.I. Masel and M. A. Shannon, "Non-equilibrium electrokinetic micro/nano fluidic mixer". Lab Chip, **8** 625–628 (2008).

15. Abgrall P. and N.T. Nguyen, "Nanofluidic devices and their applications". Analytical Chemistry, **80** 2326–2341 (2008).

16. Kim S. J., Ko S. H., Kang K. H. and Han J.Y., "Direct Seawater Desalination by Ion Concentration Polarization". Nature Nanotechnology, **5** 297–301 (2010).

17. Gendron P.-O., F. Avaltroni and K. J. Wilkinson, "Diffusion coefficients of several rhodamine derivatives as determined by pulsed field gradient-nuclear magnetic resonance and fluorescence correlation spectroscopy ". Journal of Fluorescence, **18** 1093–1101 (2008).

List of Figures

Rapid mixing is visible at both up-and downstream of the nanoporous slit. The mixing zone extends to the Y-junction on the right.

- **Figure 4**: Mixing index downstream of the nanoporous slit as function of the applied voltage at different flow rates.
- **Figure 5**: Mixing index upstream of the nanoporous slit as function of the applied voltage at different flow rates.
- **Figure 6**: The threshold voltage for the upstream mixing zone as function of the flow rate.

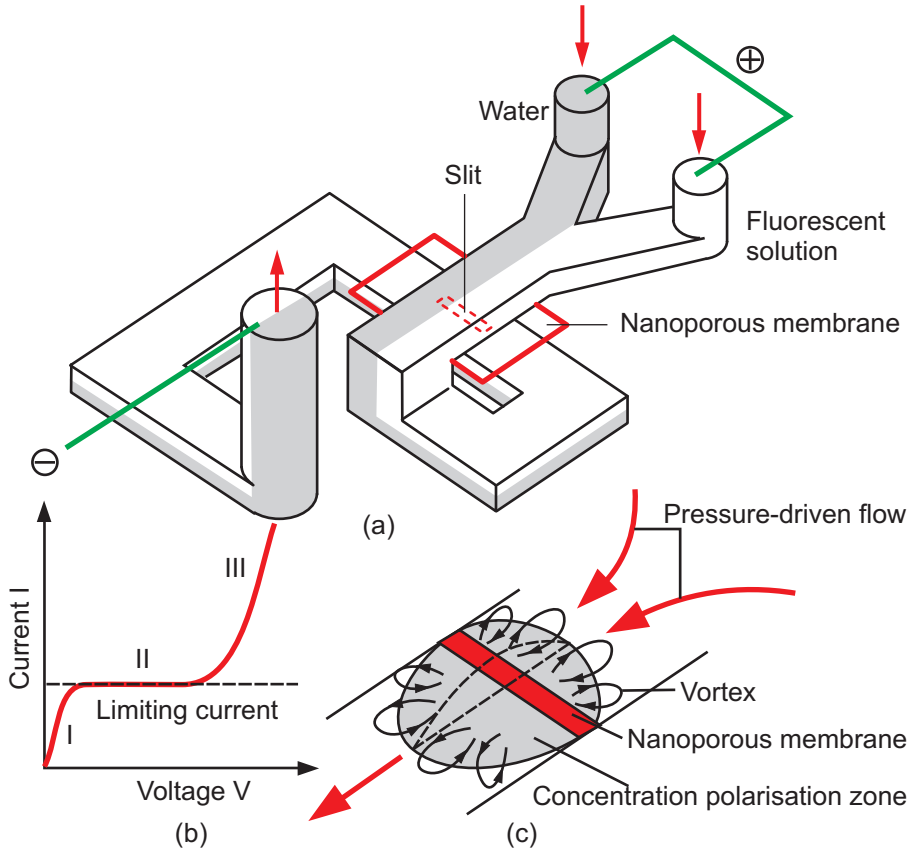

Fig. 1 Schematic concept of the pressure driven micromixer using a nanoporous membrane: (a) The flow in the mixer is driven by an external pump. The mixing channel turns and crosses the inlet. The two channels at the junction are separated by a contact slit and a nanoporous membrane. Applying a voltage across the inlet and outlet of the mixer induces a current through the nanoporous junction leading to instability in the top channel. At a high voltage, the mixing zone with strong vortices can extend to the entrance of the mixing channel. (b) Typical voltage-current curve of a cation-exchange membrane: ohmic region I, limiting region II and overlimiting region III. (c) The concentration polarisation zone above the nanoporous membrane and the induced vortices.

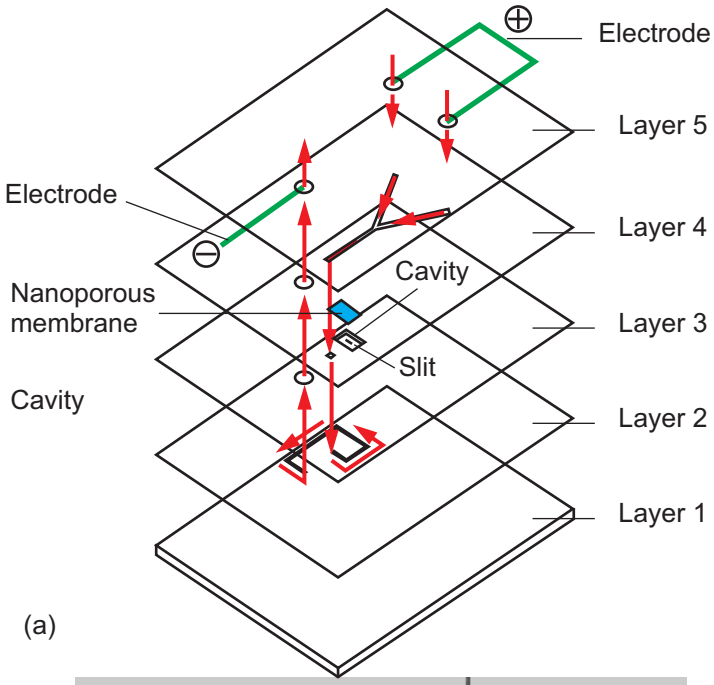

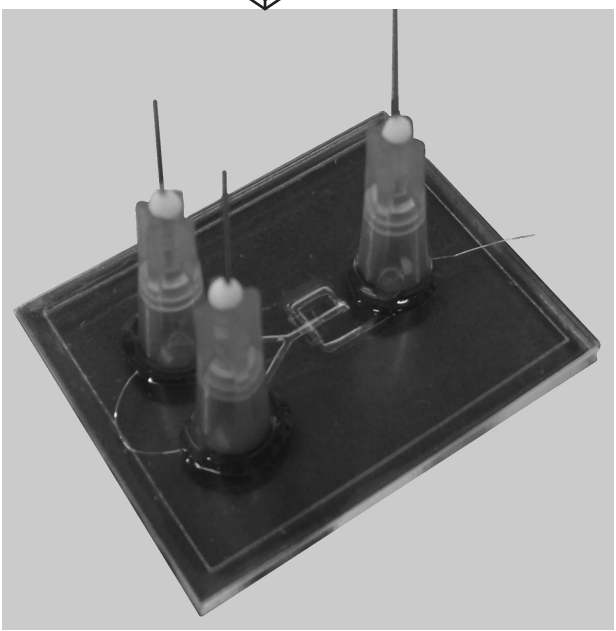

Fig. 2 The nanofluidic mixer: (a) Exploded view of the 5 layers of the mixer. Layers 2 to 5 are made of 0.25-mm thick PMMA sheets. The microchannels are cut through in layers 2 and 4. Layer 3 has a cavity to embed the rectangular nanoporous membrane. The contact slit is opened in layer 3. Layer 5 contains the access holes for the inlets and the outlet. Layer 1 is made of a 3-mm thick PMMA substrate to provide a rigid support for the entire device. (b) The assembled mixer with fluidic interconnects and platinum wires as electrodes.

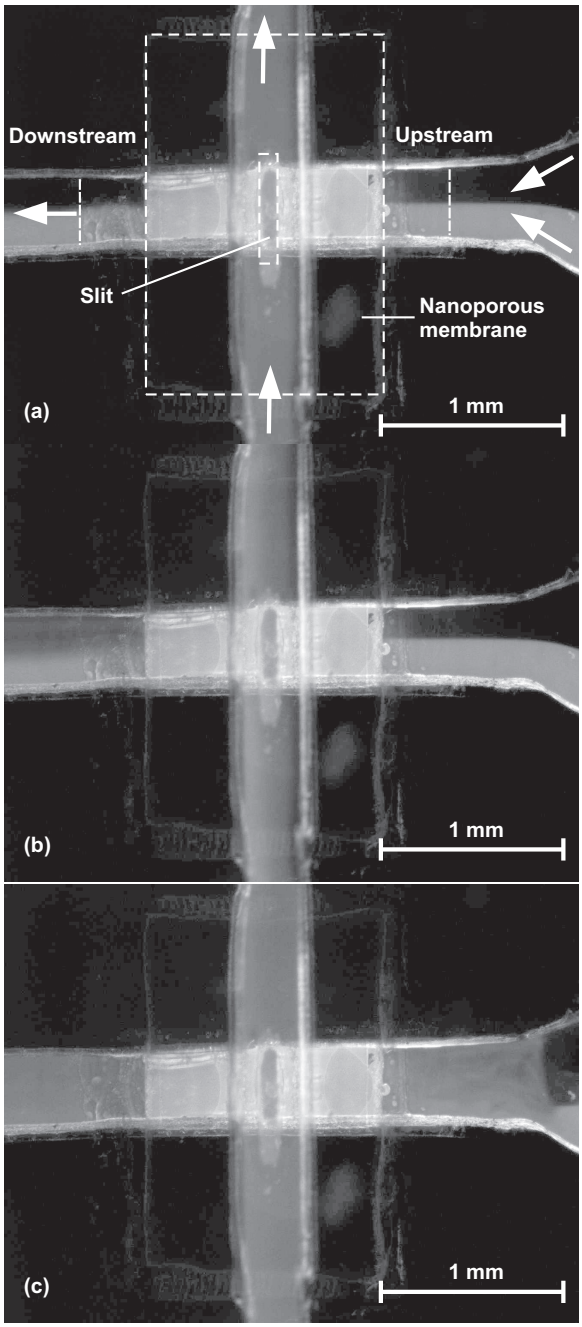

Fig. 3 Mixing behaviour at the nanofluidic junction (flow rate of 40l/min): (a) The applied voltage is zero (V=0V). DI water (dark) and fluorescent DI water (bright) meet at the Y-junction. Clear side-by-side laminar flow is observed up- and downstream of the nanoporous slit. The positions for the evaluation of mixing efficiency are labelled on the image; (b) The applied voltage is 400 V. Mixing downstream of the nanoporous slit is visible; (c) The applied voltage is 900 V. Rapid mixing is visible at both up-and downstream of the nanoporous slit. The mixing zone extends to the Y-junction on the right.

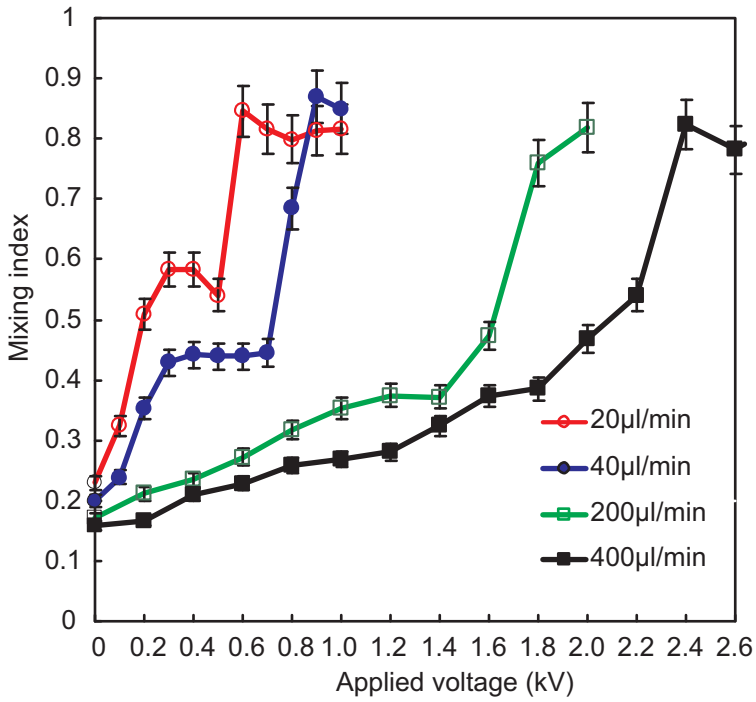

Fig. 4 Mixing index downstream of the nanoporous slit as function of the applied voltage at different flow rates.

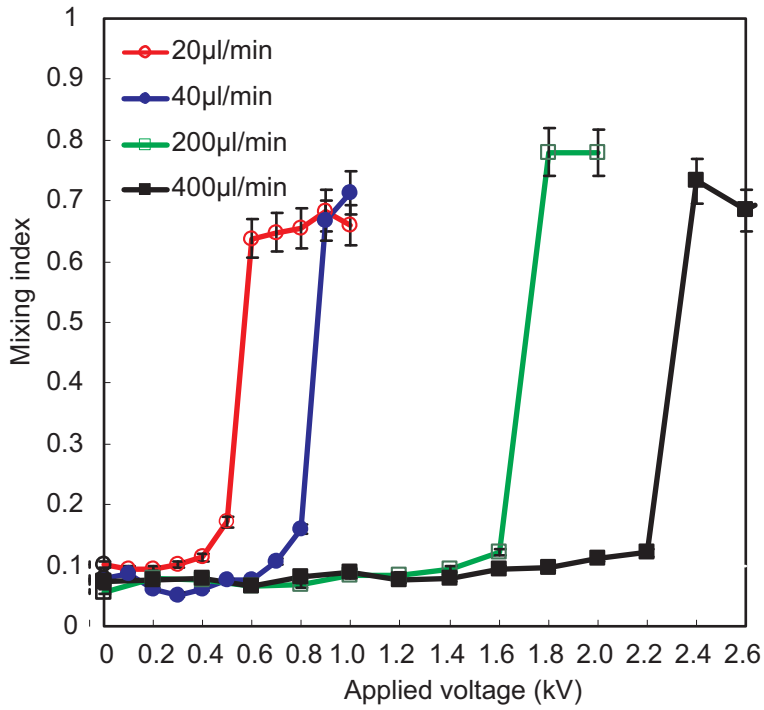

Fig. 5 Mixing index upstream of the nanoporous slit as function of the applied voltage at different flow rates.

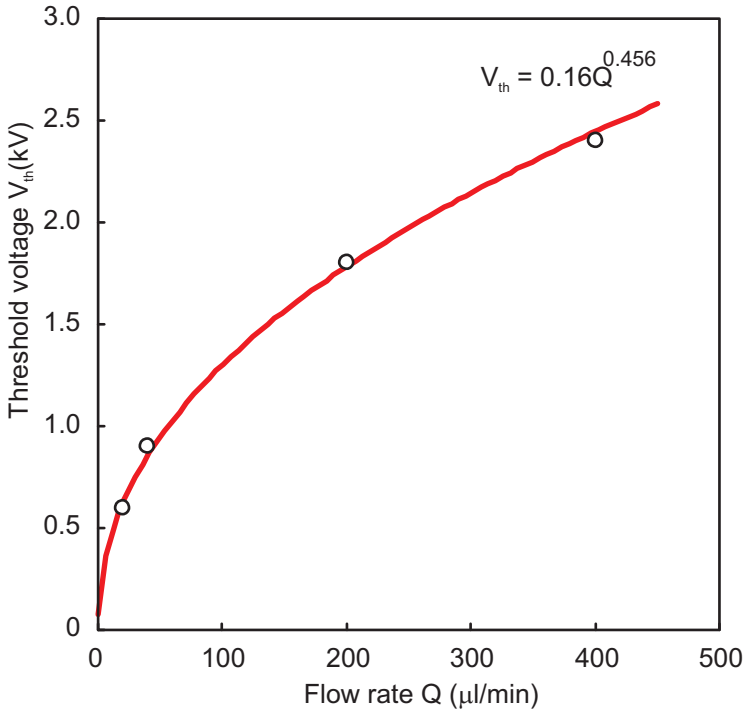

Fig. 6 The threshold voltage for the upstream mixing zone as function of the flow rate.